Carbon Nanotubes

DOI: 10.1002/anie.200902615

# High-Yield Synthesis of Ultrathin Metal Nanowires in Carbon Nanotubes**

*R. Kitaura,* R. Nakanishi, T. Saito, H. Yoshikawa, K. Awaga, and H. Shinohara**

Electrons confined in low-dimensional nanostructures show various novel physical properties owing to quantum effects that could lead to applications in nanoelectronic devices.[1] To enhance such properties, the nanostructures need to be very small and have high aspect ratios, and, thus, the synthesis of atomically thin nanowires is one of the most intriguing topics in materials science. However, such an ultrathin nanowire is always not stable because of the intrinsic structural instability and high chemical reactivity. Therefore, in addition to the high-yield controlled synthesis of such nanowires, its concomitant structural stabilization is of key importance. For this purpose, we have focused on a direct nanofilling reaction using the pseudo-one-dimensional nanospace of carbon nanotubes (CNTs).

The chemically and mechanically stable pseudo-1D hollow nanospace of CNTs ranging in size from 0.4 to 50 nm across can act as an ideal nanosized space for the self-assembly of various nanostructures. In fact, several studies on the formation of nanoclusters and nanowires in CNTs have been reported over the past couple of decades.[2] However, the formation of atomically thin nanowires inside CNTs in high yield has been difficult to date. We have developed a simple and effective synthetic procedure, whereby ultrathin nanowires of typically 1–4 atomic chains are synthesized with a high filling fraction (typically $>80\,\%$) in both single-wall CNTs (SWCNTs) and double-wall CNTs (DWCNTs). These nanowires are completely protected by surrounding walls of CNTs and are therefore free from oxidation as well as from structural decomposition under ambient air environments and even after ultrasonication in solution. This result is in marked contrast to previously reported metal nanowires, especially to the so-called single atomic nanowires, which can survive for only a very short period of time even under ultrahigh vacuum conditions.[3] Furthermore, the present method to prepare ultrathin metal nanowires in CNTs can be applied to any metal atoms that have low sublimation temperatures. Herein, we report the details on the synthesis by what we call a nanofilling reaction and on the structural characterization of ultrathin metal–nanowires in SWCNTs and DWCNTs as revealed by high-resolution transmission electron microscopy (HRTEM).

CNTs were synthesized by chemical vapor deposition and enhanced direct-injection pyrolytic synthesis (e-DIPS).[4] Metal nanowires were synthesized by placing high quality purified CNTs and metal powder into a glass tube under vacuum ($10^{-6}$ Torr) with heating. At high vacuum and high temperature, metals of low sublimation temperatures can vaporize to form atomically thin nanowires in the nanosized pseudo-1D space of CNTs. Using this simple procedure, which we call the direct nanofilling reaction, we synthesized various ultrathin metal nanowires in CNTs. Herein, we have focused on Eu metal due to its low sublimation temperature and unique magnetic properties arising from partially filled 4f orbitals.

Figure 1a shows a low magnification image of Eu nanowires encapsulated in SWCNTs (hereafter designated as Eu-nanowires@SWCNTs). In contrast with empty SWCNTs, the image clearly shows dark areas overlapping with the CNTs. In some SWCNTs, fringes arising from lattice structure of Eu metal atoms can also be recognized (Figure 1b). The energy-dispersive X-ray (EDX) spectra observed in this field show strong peaks arising from Lα and Lβ edges of the Eu atom. Therefore, we can unambiguously assign the dark areas in the SWCNTs to encapsulated individual Eu atoms. Moreover, the filling fraction of Eu atom (i.e., synthesis yield of nanowire within individual CNTs) is quite high; a rough estimation on the basis of low-magnification TEM images provides a filling fraction of Eu as high as 80–90 %. Although the evaluation of length of the nanowires is not straightforward, we have

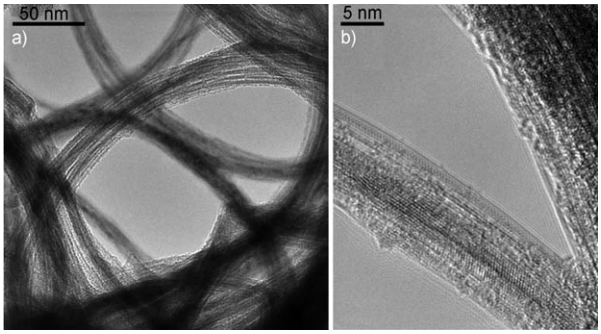


***Figure 1.*** Low-magnification TEM images of Eu-nanowire@SWCNTs.

[*] Prof. Dr. R. Kitaura, R. Nakanishi, Dr. H. Yoshikawa, Prof. Dr. K. Awaga, Prof. Dr. H. Shinohara
Department of Chemistry, Nagoya University
Nagoya 464-8602 (Japan)
Fax: (+81) 52-747-6442
E-mail: kitaura@nano.chem.nagoya-u.ac.jp
Dr. T. Saito
Nanotube Research Center, National Institute of Advanced Industrial Science and Technology, Tsukuba 305-8565 (Japan)

[**] We thank K. Sato and M. Yoshikawa (Chemical Research Laboratories, Toray Industries, Inc.) for providing us with DWCNT samples. This work was supported by a Grant-in-Aids for Specific Area.

Supporting information for this article is available on the WWW under http://dx.doi.org/10.1002/anie.200902615.

estimated that the length of metal nanowires is similar to that of CNTs used in the synthetic process because metal atoms are densely packed in CNTs and empty regions were rarely observed. Thus, the length of nanowires is estimated to be of the micrometer order, which means that the typical aspect ratio of the Eu nanowires is more than $1 \times 10^3$.

By changing the type (SWCNT, DWCNT, or MWCNT) and corresponding diameter of the CNTs used in the present reaction, we can synthesize various nanowires with a different number of chains. Figure 2a shows HRTEM images of Eu nanowires synthesized by using DWCNTs with an inner

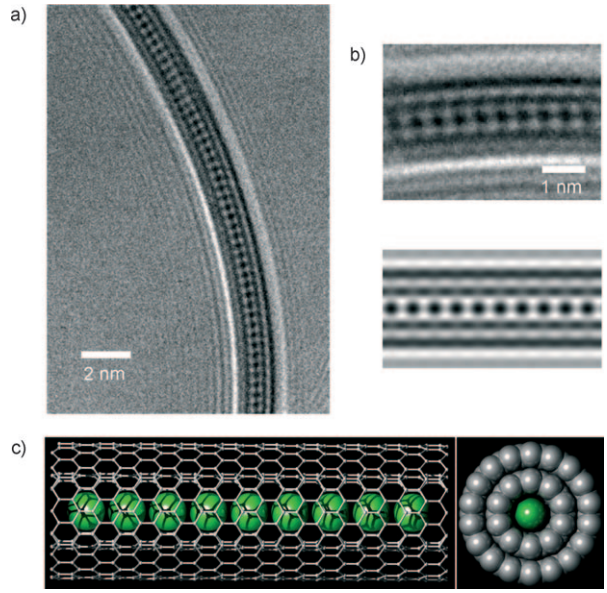


***Figure 2.*** a) HRTEM image of a single-atomic chain of Eu encapsulated in DWCNTs. b) Magnified HRTEM image and HRTEM image simulated by a multislice method at Scherzer defocus. c) Structure model of observed HRTEM image represented by a ball-and-stick model and space-filling model. The left and right pictures show the structure model perpendicular and parallel to the tube axis, respectively. Gray carbon, green europium. All image simulations were performed using the WinHREM simulation software package.

diameter of 0.76 nm. The figure clearly shows dark spots aligned in the DWCNTs in a perfectly regulated fashion. The diameter of the inner tube of the DWCNTs is only 0.76 nm, which means that the space available for encapsulation of Eu atoms is only about 0.41 nm, considering the van der Waals diameter of the inner CNT; this diameter is almost equal to the atomic size of Eu metal. Therefore, a single chain atomic wire, which is the ultimate one-dimensional nanowire, is the only possible structure in this ultranarrow space in DWCNTs. Figure 2c shows a structural model of a Eu single atomic wire encapsulated in DWCNTs. In fact, a simulated HRTEM image based on the structure model using the multi-slice method agrees well with the observed HRTEM image (Figure 2b).

For the present HRTEM observations, bulk samples of Eu-nanowire@CNTs were dispersed in organic solvent by ultrasonication for 1 hour, and the supernatant of the dispersion liquid was dropped onto copper support grids. This process allows the ultrathin single atomic Eu-wire to retain their original structure even after ultrasonication for 1 hour. Furthermore, almost identical HRTEM images to those of the as-produced Eu nanowires were observed even after exposure of the sample to air for one month. This remarkable stability of the nanowires originating from the perfect protection effect by CNTs walls is one of the most important advantages that led us to investigate their detailed properties and further fabrications in device applications. Interestingly, the interatomic distance between neighboring Eu atoms determined by direct lattice measurements was found to be 0.467 nm with a standard deviation of 0.019 nm, which is much larger than that of the bulk Eu crystal (0.39681 nm). The observed large Eu···Eu distance in the single-chain atomic wire corresponds to approximately 17% elongation relative to that of bulk crystal, which presumably originates from a significant reduction of the coordination number of Eu atom (from 12 to 2) and from a possible charge-transfer interaction between Eu atoms and CNTs.

Figure 3 shows HRTEM images of Eu nanowires formed in DWCNTs with inner-tube diameters of 1.06 and 1.54 nm. Proposed atomic structure models and simulated images

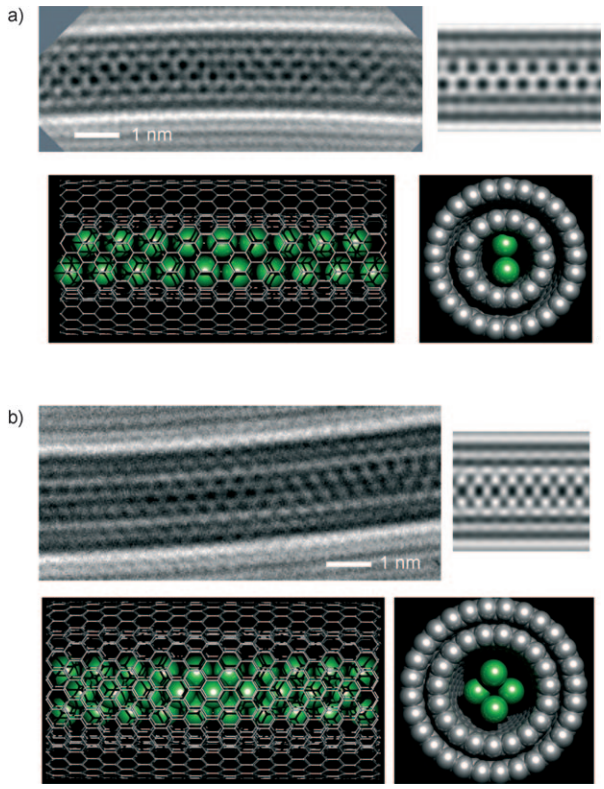


***Figure 3.*** Observed HRTEM image, simulated HRTEM image, and corresponding structure model of a) two and b) four chains of Eu atoms encapsulated in DWCNTs.

based on the structure models are also shown, and the observed and simulated images agree well in the both cases. Eu atoms form two and four chains in the DWCNTs. Direct measurement of the Eu···Eu distance from the HRTEM images provides distances of 0.437 and 0.423 nm with

  

standard deviations of 0.033 and 0.023 nm, respectively, for two and four chains of Eu atoms, respectively. These Eu···Eu distances are also longer than that of bulk the Eu crystal. The structure of Eu nanowire shown in Figure 3b is four chains of Eu atomic wires, which corresponds to a cross section of face-centered-cubic structure along the [110] axis. Since the crystal structure of bulk Eu is body-centered cubic, the packing manner of Eu atom is different from that of bulk crystal in the nanosized space of CNTs. In nanosized materials, such as nanowires with large surface area, surface energy contributes significantly to the total energy, which leads to formation of specific and unusual structures that cannot be realized in bulk crystal. As described above, one can systematically synthesize nanowires of different diameters (i.e., chains) at single atomic level by the nanofilling reaction using the nanospace of CNTs. Furthermore, our preliminary experiments show that this simple nanowire formation procedure can equally be applied to other metal atoms, such as Sm, Sr, and Yb.

Figure 4 shows a time series of HRTEM images of four-chains Eu-nanowire@DWCNTs taken at exactly the same position. Very interestingly, the close-packed Eu nanowire in Figure 4a changes into a helical structure (Figure 4c) during

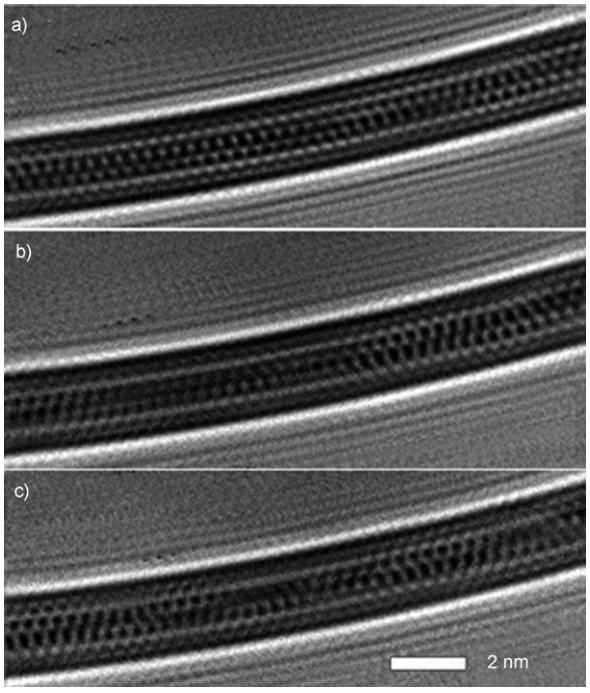


***Figure 4.*** Time series of HRTEM images of four chains of Eu atoms encapsulated in DWCNTs. A Fourier filtering treatment was applied to remove amorphous materials attached to the surface of CNTs from the image. All HRTEM images were recorded at same position.

the TEM observation. This structural transformation occurs reversibly in a time range of several seconds under irradiation of the electron beam. Theoretical investigation of a sphere filling in cylindrical space shows that spontaneous chiral symmetry breaking occurs to form helix-packed structures without causing specific intersphere interaction or sphere–cylinder interaction.[5] Therefore, the chiral symmetry breaking observed in the present Eu-nanowire@DWCNTs is essential to the confinement of metal atoms in the pseudo-one-dimensional nanospace of CNTs.

The energy difference and energy barrier for structural transformation between the closed-packed nanowire and the helical nanowire should be small, and therefore thermal fluctuation induced by electron-beam irradiation gives rise to dynamical structure transformation between the closed-packed and helical structures. This kind of structural fluctuation has been observed in Au nanoclusters, and was attributed to intrinsic properties of nanosized materials such as the coexistence of two differing phases of gold.[6] The Eu···Eu distance between nearest neighbor atoms in the series observed by HRTEM is 0.474 nm with a large standard deviation of 0.062 nm. The Eu nanowires in CNTs exhibit such a characteristic change under electron-beam irradiation that we can observe in situ structure transformation. Structural fluctuation resulting from the structural phase transition is very large, which results in the observed large Eu···Eu distance and the corresponding standard deviation. A similar helical structure of 1D atoms was also observed in suspended Au nanowires and $I_2$ molecules encapsulated in CNTs.[3,7]

The change in the specific geometrical structures of the ultrathin Eu nanowires should be accompanied by a significant change of electronic structure relative to bulk crystals. To further investigate the electronic and observed specific geometrical structure, we performed ab initio calculations based on density functional theory (DFT). We used a free single-atomic wire as a structural model, and Eu atoms (electronic configuration is $[Xe]4f^76s^2$) in the experiment were replaced by Yb atoms (electronic configuration is $[Xe]4f^{14}6s^2$) in the present calculation for computational reasons; 4f orbitals have strongly localized character and orbital overlapping of 4f orbitals between neighboring metal atoms is very small, which leads to tiny contributions from metal–metal interactions. After complete structural optimization of the free single-atomic wire, the Yb···Yb distance was 0.4346 nm and the cohesive energy was 0.14 eV. The Yb···Yb distance found experimentally in bulk crystal is 0.3879 nm (fcc structure with $a = 0.54862$ nm), which is well reproduced by the DFT calculations ($a = 0.54845$ nm in the current cell optimization calculation).

On the basis of this result, we think that one of the main reasons for the significant elongation of metal–metal distance observed in this experiment (17% elongation) is the specific geometry of the single-atomic wire. Other factors such as the effect of electron-beam irradiation and a metal–CNT interaction (such as charge transfer and orbital hybridization) may also contribute in determining the nearest-neighbor metal–metal distance. We also calculated the electronic band structure of a single-atomic wire and a zigzag wire; the results reveal that the nanosized low-dimensional structure leads to a radical modification of the electronic structure. Although bulk Yb crystal is metallic, the 6s bands do not cross the Fermi level for the nanowire, indicating that Yb single atomic wire is a semiconductor (cf. Figure S1 in the Supporting Information). Estimated band gaps for a single atomic wire and a zigzag wire are 0.91 and 0.22 eV, respectively.[8] Therefore, by carefully adjusting the diameters of CNTs used in the

  

nanofilling reaction, one can fine-tune the electronic band structure of metal nanowires synthesized.

Figure 5 shows the temperature dependence of the magnetic susceptibility of purified open-capped SWCNTs, Eu bulk crystal, and Eu-nanowire@SWCNTs with mean

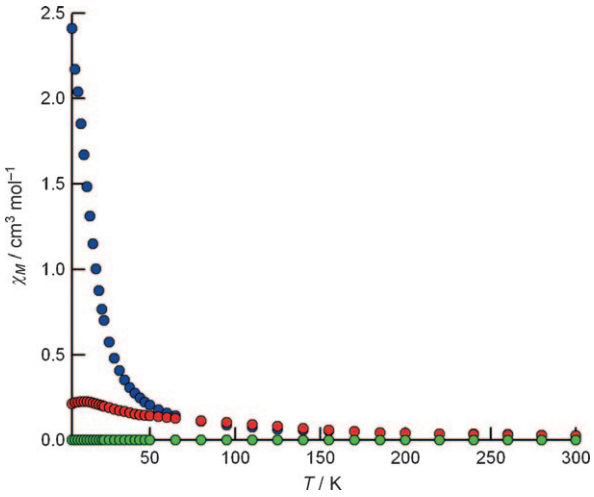


***Figure 5.*** Temperature dependence of the magnetic susceptibility of bulk Eu crystal, Eu-nanowire@SWCNTs, and purified open-capped SWCNTs. Blue: Eu-nanowire@SWCNTs; red: bulk Eu crystal; green: purified cap-opened SWCNTs.

diameter of 1.7 nm measured at a magnetic field of 1.2 T. The magnetic susceptibility of purified open-capped SWCNTs is very low, and hence we can ignore background magnetization arising from SWCNTs. The magnetization behavior of Eu nanowires is vastly different from that of Eu bulk crystals, especially below 50 K. The magnetic susceptibility of Eu nanowires is more than 10 times larger than that of the bulk Eu crystal at 4.25 K. In the case of Eu, the partially filled 4f orbital (electronic configuration of Eu is $^8S_{7/2}$) is the origin of the magnetic moment. As the 4f orbital is strongly localized, the magnetic properties of Eu compounds are well described as a localized spin system, in which interspin interactions are mediated by free electrons (RKKY interactions). In the case of the bulk crystal of Eu metal, helical spin ordering is observed below 90 K, whereby all spins in the *ab* plane align in same direction, and the spin direction in the *ab* plane rotates along the *c* axis. This helical spin ordering causes each spin alignment in the *ab* plane to cancel out, which leads to a decrease of the total magnetic moment. Because the structure and dimensionality of Eu nanowires are vastly different from those of the bulk Eu crystal, the helical spin alignment observed in bulk Eu crystal is probably incompatible with Eu nanowires. Therefore, cancelling out of spin observed in the Eu bulk crystal is also incompatible with Eu nanowires, which leads to a dramatic increase of the total magnetic moment. As described above, we can change not only the electronic structure but also the magnetic properties by changing the dimensions of the Eu metal.

In summary, we synthesized ultrathin metal (Eu) nanowires with diameters of a single atom (ca. 1.7 nm) in a very high filling fraction using the nanofilling reaction. Because the nanowires are confined within and protected by the walls of the CNTs, the nanowires resist oxidation and structural disintegration even in ambient conditions. Furthermore, the protection by CNTs enables us not only to investigate their detailed structure and properties of the nanowires but also to process the nanowires to form various kinds of electronic devices using the ultrathin nanowires. Furthermore, the present fabrication method is generally applicable to various metals that have low sublimation temperatures. In fact, our preliminary experiments show that Sm, Yb, and Sr nanowires can be similarly synthesized using the current method. The present ultrathin metal nanowires of a controlled diameter are an ideal model system to explore one-dimensional phenomena and applications as nanoconnectors for designing nanoelectronic devices. For this purpose, we are currently investigating various properties of isolated single ultrathin nanowires.

## Experimental Section

Sample preparation: As-produced CNTs were purified by vacuum annealing at 1473 K and $10^{-6}$ Torr for 12 h to remove remaining metal catalyst nanoparticles and amorphous carbon impurities. After the samples were purified, cap opening was carried out by dry-air oxidation at 823 K for 30 min. Open-capped purified CNTs and ground metal powder were placed in a glass tube under an Ar atmosphere. After vacuum heat treatment at 500 K for 1 h, the glass tube was vacuum sealed at $10^{-6}$ Torr. The glass tube was then heated at 773–873 K for 1 day in an electric furnace. The metal-encapsulating CNTs synthesized in this way were heated at 773 K for 12 h under vacuum and then washed with diluted HCl to remove residual metal atoms attached the outer surface of the CNTs.

HRTEM observations: Observations were performed on a JEM-2100F (JEOL) high-resolution field-emission gun TEM operated at 80 keV at room temperature and under a pressure of $10^{-6}$ Pa. The sample was dispersed in 1,2-dichlorobenzene by ultrasonication for 1 h, and the supernatant was dropped onto a copper grid coated with thin carbon film. The sample was vacuum treated at 473 K for 1 h to remove 1,2-dichrolobenzene before the TEM observations were carried out. HRTEM images were recorded with a charge-coupled device with an exposure time of typically 1–3 s.

Magnetic susceptibility measurements: Measurements of magnetic susceptibility were performed using a Quantum Design MPMS XL magnetometer. Prior to measurement, the samples were heated at 573 K and vacuum sealed in quartz tubes at $10^{-6}$ Torr. Samples of bulk Eu crystals were prepared under anaerobic conditions to prevent oxidation of Eu.

Density functional calculations: DFT calculations in the generalized gradient approximation (GGA) were used and a plane-wave basis set was employed with a cutoff energy of 400 eV. Interaction between the ionic cores and valence electrons was treated by the projector augmented-wave (PAW) method in the implementation of Kresse and Joubert.[9] Structure relaxation was carried out using 40 irreducible $k$ points with a coordinate $(0, 0, n/80) \times (2\pi/T)$ ($n = 0,1, \ldots 40$), where $T$ is the translational period. For the band-structure calculation, 200 irreducible $k$ points were used. The nanowires were placed on a rectangular grid separated by 1.5 nm vacuum, which results in negligible interwire interactions. Gaussian smearing with the parameter $\sigma = 0.01$ eV was applied to broaden the one-electron

  

eigenenergies. All calculations were carried out using the Vienna ab initio simulation package (VASP).[10]

Received: May 16, 2009
Revised: August 5, 2009
Published online: September 22, 2009

**Keywords:** carbon · electron microscopy · magnetic properties · nanotubes · nanowires

[1] a) J. T. Hu, T. W. Odom, C. M. Lieber, *Acc. Chem. Res.* **1999**, *32*, 435 – 445; b) W. Lu, C. M. Lieber, *Nat. Mater.* **2007**, *6*, 841 – 850; c) H. Ohnishi, Y. Kondo, K. Takayanagi, *Nature* **1998**, *395*, 780 – 783.

[2] a) P. M. Ajayan, S. Iijima, *Nature* **1993**, *361*, 333 – 334; b) P. M. Ajayan, O. Stephan, P. Redlich, C. Colliex, *Nature* **1995**, *375*, 564 – 567; c) E. Philp, J. Sloan, A. I. Kirkland, R. R. Meyer, S. Friedrichs, J. L. Hutchison, M. L. H. Green, *Nat. Mater.* **2003**, *2*, 788 – 791; d) R. Kitaura, D. Oagawa, K. Kobayashi, T. Saito, S. Ohshima, T. Nakamura, H. Yoshikawa, K. Awaga, H. Shinohara, *Nano Res.* **2008**, *1*, 152 – 157; e) R. R. Meyer, J. Sloan, R. E. Dunin-Borkowski, A. I. Kirkland, M. C. Novotny, S. R. Bailey, J. L. Hutchison, M. L. H. Green, *Science* **2000**, *289*, 1324 – 1326; f) C. Guerretpiecourt, Y. Lebouar, A. Loiseau, H. Pascard, *Nature* **1994**, *372*, 761 – 765; g) A. Govindaraj, B. C. Satishkumar, M. Nath, C. N. R. Rao, *Chem. Mater.* **2000**, *12*, 202 – 205; h) A. L. Elías, J. A. Rodriguez-Manzo, M. R. McCartney, D. Golberg, A. Zamudio, S. E. Baltazar, F. Lopez-Urias, E. Munoz-Sandoval, L. Gu, C. C. Tang, D. J. Smith, Y. Bando, H. Terrones, M. Terrones, *Nano Lett.* **2005**, *5*, 467 – 472; i) H. Muramatsu, T. Hayashi, Y. A. Kim, D. Shimamoto, M. Endo, M. Terrones, M. S. Dresselhaus, *Nano Lett.* **2008**, *8*, 237 – 240; j) R. Kitaura, N. Imazu, K. Kobayashi, H. Shinohara, *Nano Lett.* **2008**, *8*, 693 – 699; k) N. Tombros, L. Buit, I. Arfaoui, T. Tsoufis, D. Gournis, P. N. Trikalitis, S. J. van der Molen, P. Rudolf, B. J. van Wees, *Nano Lett.* **2008**, *8*, 3060 – 3064; l) R. Carter, J. Sloan, A. I. Kirkland, R. R. Meyer, P. J. D. Lindan, G. Lin, M. L. H. Green, A. Vlandas, J. L. Hutchison, J. Harding, *Phys. Rev. Lett.* **2006**, *96*, 0; m) T. Pichler, C. Kramberger, P. Ayala, H. Shiozawa, M. Knupfer, M. H. Rummeli, D. Batchelor, R. Kitaura, N. Imazu, K. Kobayashi, H. Shinohara, *Phys. Status Solidi B* **2008**, *245*, 2038 – 2041.

[3] Y. Kondo, K. Takayanagi, *Science* **2000**, *289*, 606 – 608.

[4] T. Saito, S. Ohshima, T. Okazaki, S. Ohmori, M. Yumura, S. Iijima, *J. Nanosci. Nanotech.* **2008**, *8*, 6153 – 6157.

[5] G. T. Pickett, M. Gross, H. Okuyama, *Phys. Rev. Lett.* **2000**, *85*, 3652 – 3655.

[6] S. Iijima, T. Ichihashi, *Phys. Rev. Lett.* **1986**, *56*, 616 – 619.

[7] L. H. Guan, K. Suenaga, Z. J. Shi, Z. N. Gu, S. Iijima, *Nano Lett.* **2007**, *7*, 1532 – 1535.

[8] Although the GGA method underestimates the band gap, we can still compare relative values.

[9] G. Kresse, D. Joubert, *Phys. Rev. B* **1999**, *59*, 1758 – 1775.

[10] a) G. Kresse, J. Furthmüller, *Comput. Mater. Sci.* **1996**, *6*, 15 – 50; b) G. Kresse, J. Furthmüller, *Phys. Rev. B* **1996**, *54*, 11169 – 11186.

  